Progress in Systems and Control Theory
Volume 21

Series Editor
Christopher I. Byrnes, Washington University

Control Problems in Industry

Proceedings from the SIAM Symposium on Control Problems San Diego, California July 22-23, 1994

Irena Lasiecka and Blaise Morton
Editors

1995

Birkhäuser
Boston • Basel • Berlin

Modeling the Induction Process of an Automobile Engine

P.E. Moraal[†], J.A. Cook[*], and J.W. Grizzle[‡]

October 12, 1994

Abstract

This paper adresses the problem of estimating the air charge inducted into the cylinders of a four-stroke cycle, spark ignition internal combustion engine. The first part of the paper describes a low frequency model of the induction process. Using this model, a real-time air charge estimator is constructed, based on measurements of air flow from a hot-wire anemometer located upstream of the throttle. The importance of appropriate compensation for the relatively slow air meter dynamics is described. In the second part of the paper, a more complete dynamical model is developed, incorporating intake runner acoustic and inertial effects, which is capable of describing the induction process in the individual cylinders. A potential application of this model in controlling a four-cylinder engine with variable valve timing is briefly discussed.

1 Introduction

The four-stroke cycle, spark ignition, internal combustion engine consists of a number of cylinders (usually four, six or eight in automotive applications, although ten and twelve are not unheard of) wherein reciprocating pistons transmit power via a simple connecting rod and crankshaft mechanism to the wheels. Two complete revolutions of the crankshaft comprise the following sequence of operations: The initial 180 degrees of crankshaft revolution is the intake stroke where the piston travels from top-dead-center (TDC) in the cylinder to bottom-dead-center (BDC). During this time an intake valve in the top of the cylinder is opened and a combustible mixture of air and fuel is drawn in from an intake manifold. Subsequent 180 degree increments of crankshaft revolution comprise the compression stroke, where the intake valve is closed and the mixture is compressed as the piston moves back to the top of the cylinder; the combustion stroke, when, after the mixture is ignited by a spark plug, torque is generated at the crankshaft by the downward motion of the piston caused by the expanding gas; and finally, the exhaust stroke, when the piston moves back up in the

[*]Ford Motor Company, MD 1170, P.O. Box 2053, Dearborn, MI 48121-2053

[†]Department of EECS, University of Michigan, Ann Arbor, MI 48109–2122; work supported in part by the National Science Foundation under contract NSF ECS-92-13551.

cylinder, expelling the products of combustion through an exhaust valve. This paper is concerned only with the induction process, essentially, only the first 180 degrees of the 720 degree engine cycle. The physical system is represented schematically in Figure 1, and consists of a throttle and intake manifold plenum communicating via individual passages, or runners, with the cylinder intake ports.

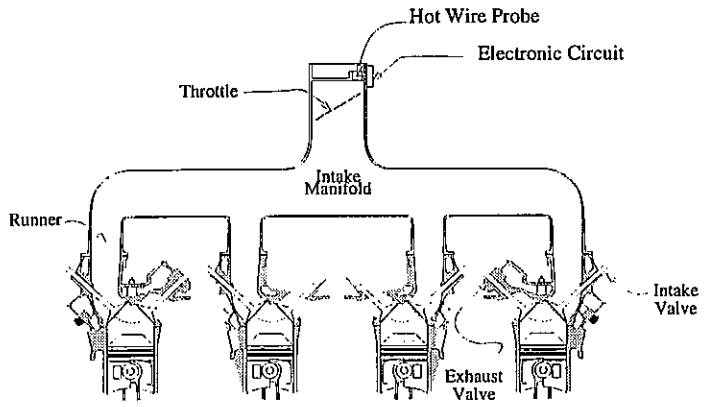

Figure 1: Schematic of Air Path in Engine.

Mathematical models of the air path in a naturally aspirated internal combustion engine have been studied for many years. The models can roughly be categorized as two types: Partial Differential Equation (PDE) models for engine component design or off-line simulaton (see e.g. [3, 6]), and lumped parameter (plenum) models for control law design [7, 8]. The former are typically more accurate than the latter, but also much more complex and unsuited for real-time applications.

In the following sections, two system models will be developed. The first is a simple plenum model in which the intake manifold pressure is assumed to be uniform, and equal to the pressure at the inlet port. Such a model is unable to capture fast dynamics, acoustic or inertial effects that occur during one intake stroke, but is particularly appropriate for real-time estimation of cylinder air charge and air-fuel ratio (A/F) control, as is illustrated here. The second model that will be examined is an attempt to describe the induction process in more detail and with greater accuracy, without resorting to PDE's. The model is based on a plenum model to the extent that the pressures in the intake manifold and cylinders are assumed to be uniform. Additionally, a pressure at the intake valve between the runner and the cylinder is defined which is made up of the manifold pressure and spatially dependent terms describing pressure fluctuations due to acoustic and inertial effects at the inlet port. In this case, the mass flow into the cylinder is determined not by an average manifold

pressure, as in the plenum model, but by the inlet port pressure.

Nomenclature:

A : runner pipe cross section (in^2)
B : cylinder bore (in)
CAC: cylinder air charge per induction event (lbm)
Lift : valve lift dependent intake cross section (in^2)
MAF: mass air flow (lbm/sec)
N : engine speed (RPM)
R : specific gas constant (=53.39 $\frac{ft \cdot lb_f}{^\circ R \cdot lb_m}$)
S : cylinder stroke (in)
T_i : inlet air temperature (°R)
T_{EC} : engine coolant temperature (°R)
V : volume (cubic inches)
c : velocity of sound (in/sec)
d : differential pressure coefficient
l_r : runner length (inches)
m : mass (lbs)
$\dot{m}$: mass flow rate (lbs/sec)
n : number of cylinders
p : pressure (psi)
t : time (seconds)
v_p : piston velocity (in/sec)
v_r : runner gas velocity (in/sec)
α^i : characteristic air charge coefficient for cylinder i
γ : air meter time constant
ϕ : throttle position angle (degrees)
θ : crank angle (degrees)

Subscripts:
man : manifold
cyl : cylinder
amb : ambient

2 Four-Cylinder Engine Air Flow Model

2.1 Background

Precise control of air-fuel ratio (A/F) to the stoichiometric value is necessary to minimize exhaust emissions in vehicles employing a three-way catalytic converter (TWC). This is illustrated in Figure 2, where the conversion efficiencies for HC, CO and NO_x provided by the TWC are plotted against exhaust gas air-fuel ratio (A/F). It can be seen that there is only a very narrow range of A/F

near the stoichiometric value of 14.64 over which high simultaneous conversion efficiencies may be attained.

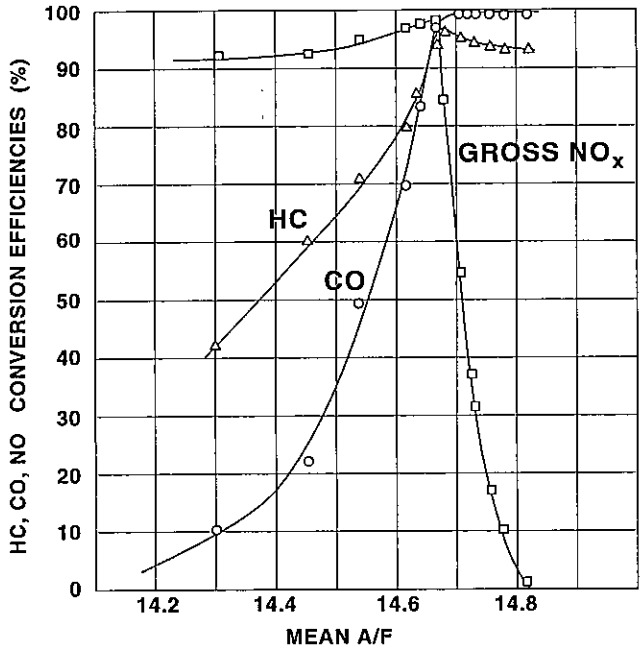

Figure 2: TWC Conversion Efficiency Characteristics.

In vehicles equipped with electronically controlled fuel injection systems, A/F control has two principle components: a closed-loop portion in which a signal related to A/F from an exhaust gas oxygen (EGO) sensor located in the exhaust stream of the engine is fed back through a digital controller to regulate the fuel injection pulse width, and an open-loop, or feedforward portion in which injector fuel flow is controlled in response to a signal from an air flow meter. A block diagram of this control structure is illustrated in Figure 3. It can be appreciated that the feedback, or closed-loop portion of the A/F control system is fully effective only under steady-state operating conditions due to the significant system delay between the induction of an air and fuel charge into a cylinder and the subsequent appearance, many engine cycles later, of that A/F at the EGO sensor. Additionally, a reliable EGO sensor signal is available only after the sensor has attained a stabilized operating temperature, inhibiting closed-loop A/F control immediately upon starting the engine. Under these conditions the feedforward portion of the controller is particularly important.

This subsection describes the feedforward component of A/F control. In

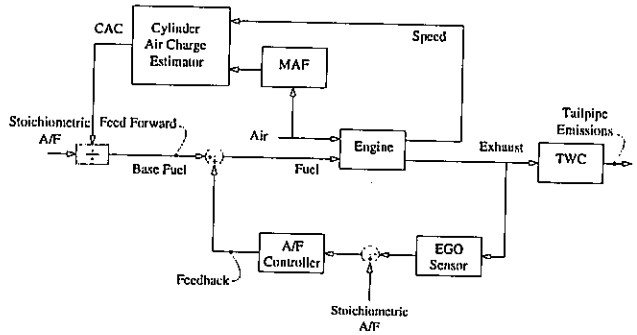

Figure 3: A/F Control Loop Illustrating Feed Forward and Feedback Elements.

particular, an implementation of a nonlinear air charge estimator is developed. The estimator is required to predict the air charge entering the cylinders downstream of the intake manifold plenum from available measurements of air mass flow rate upstream of the throttle. This air charge estimate is used to form the base, or open-loop, fuel calculation. A practical problem is encountered in that the hot-wire anemometer used to measure air flow mass rate has non-negligible dynamics. Indeed, the time constant of this sensor is often on the order of an induction event for an engine speed of 1500 revolutions per minute, and is only about four to five times faster than the dynamics of the intake manifold. Taking these dynamics into account in the air charge estimation algorithm can significantly improve the accuracy of the algorithm and have substantial benefits for reducing emissions.

2.2 Basic model

The air path of a typical engine is depicted in Figure 3. An associated lumped parameter phenomenological model, suitable for developing an on-line cylinder air charge estimator [2] is now described. Let p_{man}, V, T and m be the pressure in the intake manifold (psi), volume of the intake manifold and runners (in^3), temperature ($^\circ$R) and mass (lbm) of the air in the intake manifold, respectively. Invoking the ideal gas law, and assuming that the manifold air temperature is slowly varying leads to

$$\frac{d}{dt}p_{man} = \frac{RT}{V}[MAF_a - Cyl(N, p_{man}, T_{EC}, T_i)], \qquad (1)$$

where MAF_a is the actual mass air flow metered in by the throttle, and the expression $Cyl(N, p_{man}, T_{EC}, T_i)$ represents the average instantaneous air flow pumped out of the intake manifold by the cylinders, as a function of engine speed, N (RPM), manifold pressure, engine coolant temperature, T_{EC} ($^\circ R$), and

air inlet temperature, T_i ($^\circ R$). It is assumed that both $Cyl(N, p_{man}, T_{EC}, T_i)$ and MAF_a have units of lbm/sec.

The dependence of the cylinder pumping or induction function on variations of the engine coolant and air inlet temperatures is modeled by [3]

$$Cyl(N, p_{man}, T_{EC}, T_i) = Cyl(N, p_{man}) \sqrt{\frac{T_i}{T_i^{\text{mapping}}}} \frac{T_{EC}^{\text{mapping}} + 2460}{T_{EC} + 2460}, \quad (2)$$

where the superscript 'mapping' denotes the corresponding temperatures at which the function $Cyl(N, p_{man})$ is determined, based on engine mapping data.

Cylinder air charge per induction event, CAC, can be determined directly from (1). In steady state, the integral of the mass flow rate of air pumped out of the intake manifold over two engine revolutions, divided by the number of cylinders, is the air charge per cylinder. Since engine speed is nearly constant over a single induction event, a good approximation of the inducted air charge on a per cylinder basis is given by

$$CAC = \frac{120}{nN} Cyl(N, p_{man}, T_{EC}, T_i) \text{ lbm}. \quad (3)$$

The final element to be incorporated in the model is the mass air flow meter. The importance of including this was demonstrated in [2]. For the purpose of achieving rapid on-line computations, a simple first order model will be used:

$$\gamma \frac{d}{dt} MAF_m + MAF_m = MAF_a \ , \quad (4)$$

where MAF_m is the measured mass air flow and γ is the time constant of the air meter. Substituting the left hand side of (4) for MAF_a in (1) yields

$$\frac{d}{dt} p_{man} = \frac{RT}{V} \left[\gamma \frac{d}{dt} MAF_m + MAF_m - Cyl(N, p_{man}, T_{EC}, T_i) \right] \quad (5)$$

To eliminate the derivative of MAF_m in the above equation, let $x = p_{man} - \gamma \frac{RT}{V} MAF_m$. This yields

$$\frac{d}{dt} x = \frac{RT}{V} \left[MAF_m - Cyl(N, x + \gamma \frac{RT}{V} MAF_m, T_{EC}, T_i) \right]. \quad (6)$$

Cylinder air charge is then computed from (3) as

$$CAC = \frac{120}{nN} Cyl(N, x + \gamma \frac{RT}{V} MAF_m, T_{EC}, T_i) \ . \quad (7)$$

Note that the effect of including the mass air flow meter's dynamics is to add a feedforward term involving the mass air flow rate to the cylinder air charge computation. When $\gamma = 0$, (6) and (7) reduce to an estimator which ignores the air meter's dynamics, or equivalently, treats the sensor as being infinitely fast.

2.3 Model Discretization and Validation

For implementation in the embedded engine control microprocessor, the estimator must be cast in discrete form. In automotive engine control, event based sampling synchronized with the four-stroke cycle is not uncommon [8]. For illustration purposes, the discretization will be carried out here for a V8; the modifications required for other engine configurations will be evident. In this case, one induction event occurs every 90 degrees of crankshaft revolution. Let k be the recursion index and let Δt_k be the elapsed time in seconds per 45 degrees of crank-angle advancement, or $\frac{1}{8}$ revolution; that is, $\Delta t_k = \frac{7.5}{N_k}$ sec., where N_k is the current engine speed in RPM. Then (6) can be Euler integrated as

$$\begin{aligned} x_k = \ & x_{k-1} + \Delta t_k \tfrac{RT_{k-1}}{V} \cdot \\ & \cdot \left[MAF_{m,k-1} - Cyl(N_{k-1}, x_{k-1} + \gamma \tfrac{RT_{k-1}}{V} MAF_{m,k-1}, T_{EC}, T_i) \right] \end{aligned} \quad (8)$$

The cylinder air charge is calculated by

$$CAC_k = 2\Delta t_k Cyl(N_k, x_k + \gamma \frac{RT_k}{V} MAF_{m,k}, T_{EC}, T_i) \ , \quad (9)$$

and needs only be computed once per 90 crank-angle degrees.

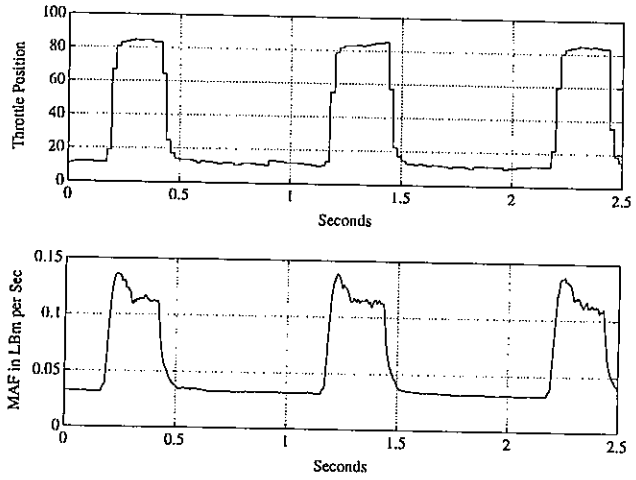

Figure 4: Engine operating conditions at nominal 1500 RPM.

The accuracy of the cylinder air charge model can be easily validated on an engine dynamometer equipped to maintain constant engine speed. Apply very rapid throttle tip-ins and tip-outs as in Figure 4, while holding the engine speed

constant. If the model parameters have been properly determined, the calculated manifold pressure will accurately track the measured manifold pressure. Figure 5 illustrates one such test at 1500 RPM.

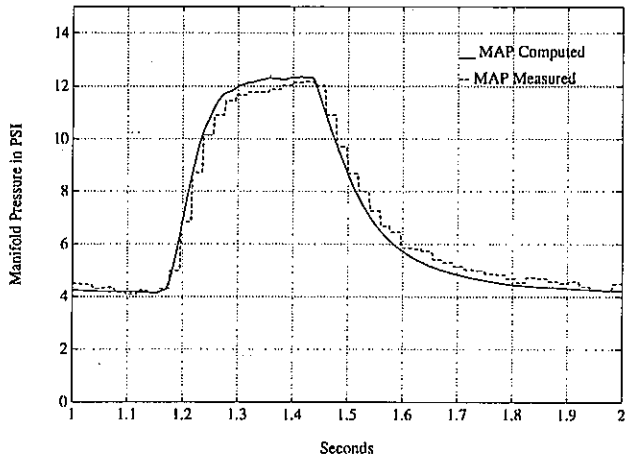

Figure 5: Comparison of measured and computed manifold pressure.

3 Individual Cylinder Induction Model

3.1 Background

In the previous section, it was assumed that the cylinder pumping map, $Cyl(N, p_{man})$, is valid and equal for all cylinders. In reality, however, due mainly to the manifold geometry, the breathing characteristics could differ significantly between individual cylinders. The resulting differences in torque production per cylinder adversely affect the smoothness of the engine operation. Since conventional engines with cam driven valve trains do not offer the control authority necessary to deal with this problem on a cylinder to cylinder basis, it has not been studied in great detail. However, with the development of advanced engine designs, featuring individually controlled valve actuators, thus introducing additional degrees of freedom, the study of this phenomenon becomes worthwhile. In fact, it becomes worthwhile for an additional reason: While a camshaft can be ground to great precision, thus ensuring equal operation of all intake valves, this may no longer be true for valve trains with individual actuators. Unavoidable variability in individual actuator characteristics may actually exacerbate the problem of air charge maldistribution.

In this section, a more detailed dynamic model of the induction process in a four-cylinder engine, capturing potential air charge maldistribution, is developed. The interaction between manifold pressure and cylinder pressure is described in terms of throttle position, individual valve timing and lift profile, engine speed and engine dependent geometric characteristics. The primary objective is to obtain a model which may be used in a real-time model-based control strategy of valve-timing in a variable valve-timing (VVT) engine. Hence, the model must be reasonably accurate, capturing the main dynamics, yet be as simple as possible (in the sense that the number of states in the dynamical model should be kept to a minimum). The work presented is an initial study, providing a basis for the control of an engine with variable valve timing. The issue of control of internal exhaust gas recirculation (EGR) is not addressed.

The model obtained here is compared to actual engine data taken at wide open throttle over a range of engine speeds. Although it is a physically based model involving parameters that can be determined a-priori (such as the dimensions of the intake system), other parameters describing flow losses, resonant frequencies, etc. have to be determined experimentally for each given engine configuration.

3.2 Model Development

The model we propose here is based on a plenum model: The pressures in the intake manifold and cylinders are assumed to be uniform. However, we depart from the plenum model by defining an inlet pressure (i.e., pressure at the inlet valve between runner and cylinder), which is comprised of the runner pressure and terms describing additional spatially dependent pressure fluctuations due to acoustic effects as they occur at the inlet port. The reason for doing so is that the mass flow across a valve or restriction from one plenum into another is determined by the ratio of upstream and downstream pressure on both sides of the valve. In particular, the mass flow into the cylinder is determined not by an average runner pressure (as assumed in the "plenum" model), but by the pressure at the inlet port. Rather than developing a spatially distributed pressure model for the runner, or even the entire intake system (as is done in the unsteady compressible flow dynamical models) and evaluating that model at the inlet port, it will be shown that it suffices to approximate such a model at the inlet port only. That way, a low-dimensional model can be utilized which does take inertial and acoustic effects into account. Such a simplification comes at the cost of decreased accuracy and possibly the loss of some physical insight in the resulting model, however, such compromises are inevitable.

The main dynamic phenomena that occur in the intake system, and which are not captured in a simple plenum model, will first be described.

When the intake valve is open, the system acts as a *Helmholtz resonator* where the driving force is a function produced by the downward piston motion, and the gas in the runner moves against the stiffness of the gas in the cylinder.

The mechanical analogue of this type of resonance is the spring-mass-damper system where the spring is the compressibility of the air in the cylinder, the mass is the air in the runner pipe and the damper is the wall friction of the gas moving through the runner pipe. In a first approximation we will model this mode of vibration as a constant coefficient Helmholtz resonator with effective volume the mean cylinder volume during the induction stroke. For that case the natural frequency is given by [9]:

$$\omega_h = \sqrt{\frac{2Ac^2}{l_r V_c}}\sqrt{\frac{r-1}{r+1}}, \tag{10}$$

where r is the compression ratio. Of course, for a better approximation, one should incorporate the time-varying cylinder volume and a speed dependent (nonlinear) wall friction term. However, it was found that the constant coefficient model already gives reasonable agreement with experimental data.

It is generally agreed that the effects of this type of resonance are noticeable only during one inlet stroke and don't persist into the the following induction event. This is an important observation in that the resonator can be modeled by a forced second order differential equation with *known* initial conditions at the beginning of each induction stroke.

The downward motion of the piston first creates a pressure drop at the inlet port, which accelerates the mass of air in the inlet runner. Later in the induction stroke, the opposite effect occurs: as the piston decelerates, approaching BDC (bottom dead center), and the intake valve closes against the moving gas, a pressure rise, due to the inertia of the moving gas, occurs at the inlet port. This phenomenon is known as *induction ram* [1]. The pressure rise Δp_{ram} at the inlet port can be calculated from:

$$\Delta p_{ram} A = \rho m \dot{v}_r,$$

where m and v_r are mass and velocity of the air in the runner respectively, A is the runner cross section and ρ is a flow geometry dependent constant which is to be determined experimentally. Note that we here conveniently ignore the fact that the local velocity of the air in the runner actually has a spatial dependence: v_r refers to the mean velocity. It should be noted that the above equation is valid only for small enough runners and engine speeds where the entire mass of air in the runner is accelerated within one induction event.

The Helmholtz resonator effect may now be tied in with the induction ram effect by modeling the unknown runner gas velocity v_r as the the solution of the differential equation:

$$\ddot{q} + 2\xi_h \omega_h \dot{q} + \omega_h^2 q = \frac{\pi B^2}{4A}\omega_h^2 v_p \tag{11}$$

with initial conditions $q(0) = \dot{q}(0) = 0$, where ω_h is the natural frequency of the resonator and ξ_h the damping ratio. The DC-gain $\frac{\pi B^2}{4A}$ represents the fact

that, in the steady state case with a constant piston velocity, the ratio of gas velocities in runner and cylinder equals the inverse ratio of their respective cross sections. The piston velocity v_p for a cylinder with stroke S is given by

$$v_p(\theta) = \frac{2\pi \mathrm{N}}{120} S \sin\theta.$$

When the intake valve is closed, the runner pipe resonates as a *quarter wave organ pipe* [9]. Once the intake valve opens again, the standing wave pattern is disturbed and the pressure fluctuation caused by it seems to have little effect on the induction process. Its main contribution is in high frequency (relative to the piston frequency) perturbations of the manifold pressure trace and will be ignored in this model.

We can now define the *inlet pressure* as $p_{in} = p_{man} + \Delta p_{ram}$, i.e., the manifold pressure plus superimposed pressure fluctuations due to the effects described above. Again, the inlet pressure is to be interpreted as the approximation of a spatially distributed pressure model, evaluated at the location of the inlet port.

The actual model is then developed as follows: starting from the ideal gas law, $pV = mRT$, the time rate of change of pressure for a constant volume plenum (such as the intake manifold and inlet runners) is derived as:

$$\dot{p} = \frac{1}{V} RT\dot{m}, \tag{12}$$

whereas for a variable volume plenum (such as the cylinders) it is given by:

$$\dot{p} = \frac{1}{V} RT\dot{m} - \frac{1}{V^2} mRT\dot{V} = \frac{1}{V}(RT\dot{m} - p\dot{V}). \tag{13}$$

The cylinder volume and time rate of change of volume for a typical 1.8L 4-cylinder engine are given by:

$$V_{cyl}(\theta) = 12.28(1-\cos(\theta)) + 2.44 \tag{14}$$

$$\dot{V}_{cyl}(\theta) = 1.286\sin(\theta)\cdot \mathrm{N}, \tag{15}$$

where the crank angle θ varies with time and engine speed as:

$$\theta = (\frac{\mathrm{N}}{60}\cdot t \cdot 360°) \mathrm{mod}\ 720°. \tag{16}$$

The mass flow rate across the throttle is modeled as

$$\dot{m} = A(\phi)\cdot d(p_1, p_2) \tag{17}$$

where

$$A(\phi) = 0.00028(-0.2215 - 2.275\phi + 0.23\phi^2)$$

$$d(p_1,p_2) = \begin{cases} 1 & \text{if } \frac{p_1}{p_2} \in [0, 0.5] \\ 2\sqrt{\frac{p_1}{p_2} - (\frac{p_1}{p_2})^2} & \text{if } \frac{p_1}{p_2} \in [0.5, 1] \\ -d(p_2, p_1) & \text{if } \frac{p_1}{p_2} > 1 \end{cases}$$

The function A expresses the geometric flow characteristics for the throttle and runner valves as a polynomial in the valve angle, ϕ, based on regressed engine data. The differential pressure function $d(p_1, p_2)$, though defined with two arguments, is a function of the ratio $\frac{p_1}{p_2}$ only. Two flow regimes are possible: If the pressure ratio across the flow area is greater than the critical ratio (about 0.5 for air), a sonic (or choked flow) condition exists, and the mass flow rate is a function *only* of the flow geometry ($d(p_1, p_2) = \pm 1$). Otherwise it is modified by the differential pressure ($-1 < d(p_1, p_2) < 1$).

For the mass flow into a cylinder, equation (17) would be replaced by:

$$\dot{m} = \alpha(\theta) \cdot \text{Lift}(\theta) \cdot d(p_1, p_2), \tag{18}$$

where $\alpha(\theta) = \alpha^i$ if $\theta \in [(i-1) \cdot 180°, i \cdot 180°)]$, $i = 1, \ldots, 4$, and $\text{Lift}(\theta) = 0.14 \sin^2 \theta$, (an approximation based on regressed engine data), which describes the geometric flow characteristics across the intake valve for each cylinder as a function of crank angle θ, scaled by the characteristic air charge coefficient α^i. (With no loss of generality, a firing order 1-2-3-4 is assumed.) The expression given for the valvelift implies that there is no overlap of individual intake lift profiles. Although this is not true for conventional valve trains, it will be seen later that this simplification has hardly any effect on the model accuracy. Of course, this would be quite different for an 8 cylinder engine, where intake valve overlap is very significant.

A model of the pressure dynamics for the 4-cylinder engine is then derived as follows: The pressure rate equation for the intake manifold plenum is expressed as the difference between the ingress mass flow rate through the primary throttle and the egress mass flow rate into the the cylinder through the intake valve. The pressure rate for the cylinders is given as a function of ingress mass flow from the manifold and time-varying cylinder volume, consistent with (13). It is assumed that there is negligible overlap of exhaust and intake valve timing, so that the exhaust system does not have to be included in the model. A comparison with actual data from an engine with a conventional valve train shows that this is indeed a reasonable assumption. The state space description of the air flow model is now given as:

$$\begin{aligned} \dot{p}_{man} &= \frac{RT}{V_{man}} \left[A(\phi) \cdot d(p_{man}, p_{amb}) - \alpha(\theta)\text{Lift}(\theta) d(p_{cyl}, p_{in}) \right] \\ \dot{p}_{cyl} &= \frac{1}{V_{cyl}(\theta)} \left[RT\alpha(\theta)\text{Lift}(\theta) d(p_{cyl}, p_{in}) - \dot{V}_{cyl}(\theta) p_{cyl} \right] \\ y &= p_{man}, \end{aligned} \tag{19}$$

where

$$p_{in} = (1 + \frac{V_r \rho \dot{q}}{RTA_r}) p_{man} \tag{20}$$

and q is the solution of the differential equation (11) with initial conditions periodically reset: $\dot{q}(0 \bmod 180°) = q(\bmod 180°) = 0$. In equation (19), $\alpha(\theta)$ denotes the air charge coefficient α^i when cylinder i is performing the induction stroke at the given time θ in the engine cycle. It is expected that such a model, although only of second order, will still capture the effects of induction ram and Helmholtz resonance with reasonable accuracy, due to the postulated model of the inlet pressure.

This model was evaluated for a 4-cylinder engine with the following technical specifications:

manifold volume	1 dm^3	runner volume	0.5 dm^3
bore	80.6 mm	runner length	35 cm
stroke	88.0 mm	compression ratio	10 : 1
exhaust valve opening	44° BBDC	exhaust valve closing	10° ATDC
intake valve opening	8° BTDC	intake valve closing	46° ABDC
valve diameter	32 mm	max. intake valve lift	8.1 mm

(BBDC: Before bottom dead center, ATDC: After top dead center, etc.)

A comparison of the model with actual engine data at 1500 RPM and 3000 RPM, wide open throttle is shown in Figures 6 and 7 respectively, where the pressure traces of intake manifold and a cylinder during the induction stroke are shown. The values of the various model parameters were determined as: Helmholtz resonator frequency and damping ratio: $\omega_h = 2\pi\ 190$; $\xi_h = 0.15$,

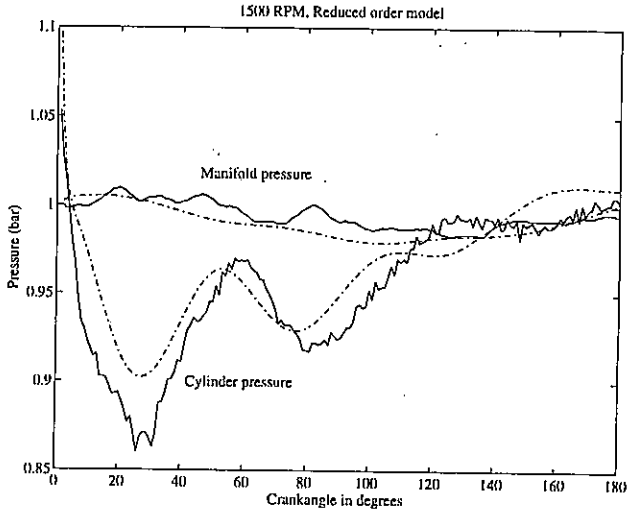

Figure 6: *Model comparison at 1500 RPM: Actual engine (solid lines) and model (dotted lines)*

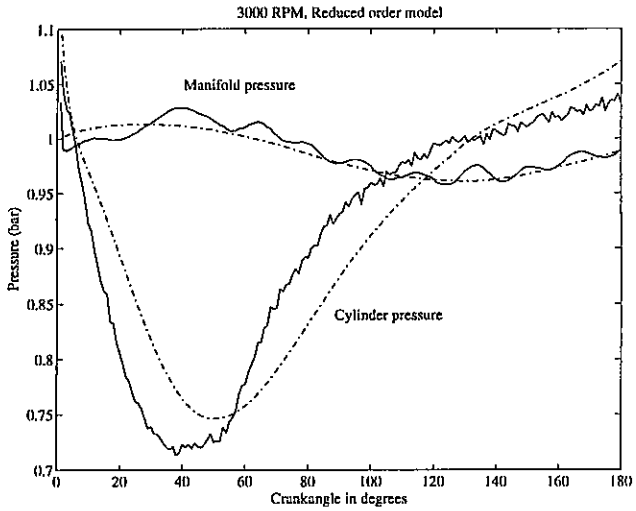

Figure 7: *Model comparison at 3000 RPM: Actual engine (solid lines) and model (dotted lines)*

and $\rho = 0.04$. Figures 6 and 7 show that the proposed model captures most of the dynamic effects that occur during induction, although some of the faster dynamics in the manifold pressure are not adequately modeled. It is also evident that the effects of valve timing overlap can indeed be neglected.

3.3 Estimation of air charge maldistribution

The above model can be augmented with four states, $\alpha := (\alpha^1, \ldots, \alpha^4)^T$, having no dynamics, i.e., $\dot{\alpha} = 0$, resulting in a 6-state dynamical system.

Since, in production engines, there are neither in-cylinder pressure sensors, nor individual runner air flow meters, the maldistribution coefficients have to be determined using other, measured variables. It was shown in [4] that the problem of determining individual cylinder air charge, equivalent to estimating the initial conditions of the four auxiliary state variables α, can be solved using measurements of the manifold pressure only. With α known, the differential equation for the cylinder pressure may be integrated starting from a known initial condition (namely, the residual exhaust gas pressure at the end of the exhaust stroke). The total air charge into the cylinder is proportional to the cylinder pressure at the end of the intake stroke. In fact, when one is primarily interested in determining the amount of air charge maldistribution, knowledge of the parameters α is sufficient, since they are a direct indication of the amount of air charge maldistribution.

In [4], the design of such a nonlinear observer is described, along with some simulations. The particular observer used is based on a new approach to observer design for nonlinear discrete-time systems, presented in [5]. The proposed method relies on block processing the outputs of the original discrete-time system, by grouping a predetermined number of past measurements, and developing an explicit relation between the system's states and the augmented output. This relation is termed a "state-to-measurement map", which, under suitable conditions, can be inverted in order to obtain state information from the given measurements. The observer problem is thus viewed as one of solving a sequence of nonlinear equations. The difficulty in this approach lies, of course, in the inversion process, which will rarely ever be possible in closed form, but rather has to be done numerically. Several schemes were developed to efficiently implement this numerical inversion. The computationally most efficient observer uses Broyden's method in the nonlinear inversion. For details, the reader is referred to [4] and [5].

3.4 Simulation Results

In the simulation results shown here, the vector of maldistribution parameters α was set to [0.9 0.83 1.17 0.77]. When perfect knowledge of the model and no measurement noise is assumed, then the observer converges in a few steps for a large range of values for α. When measurement noise is present, the observer can be made to perform satisfactorily by pre-filtering the measurements [4]. In Fig 8, it is shown that the observer is insensitive to variations in the assumed initial cylinder pressure: When $p_c(0)/\text{psi}$ has a random distribution $\mathcal{N}(16, 0.45)$, then the observer error still converges to near zero.

Finally, for modeling errors of $\pm$ 10% of the parameters ω_h, ζ_h, ρ, p_{amb} or T, simulations showed that the observer error typically converges to a biased value of at most $\pm$ 10% such that, although the absolute cylinder air charge cannot accurately be computed, one still obtains a measure of the *relative* air charge maldistribution between cylinders.

The fact that, even if modeling errors are present, the observer still gives a good estimate of the *relative* air charge maldistribution may be exploited in a simple control structure. If the valve timing can be controlled directly, which is the case in engines with variable valve timing, then the function $\text{Lift}_i(\theta)$, which governs air-intake, could be scaled by $\frac{1}{\hat{\alpha}^i}\frac{1}{4}\sum_{j=1}^{4}\hat{\alpha}^j$, i.e., the valve lift for each cylinder is scaled by the inverse of the estimated maldistribution coefficient such that the average scaling factor equals one. In Figure 9, it is seen that such an observer based control stategy can indeed eliminate air charge maldistribution: the plot shows the cylinder pressure in each of the four cylinders at the end of their respective induction stroke, which is directly proportional to the amount

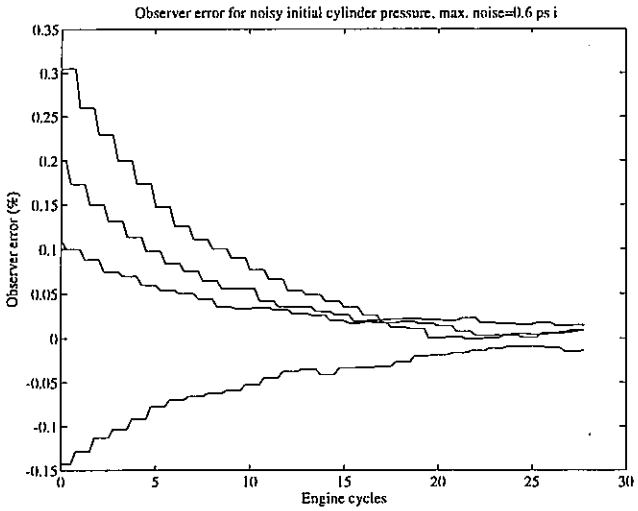

Figure 8: Observer error for random initial cylinder pressure

of air inducted during that intake stroke. The controller is switched on after an initial period of 50 engine cycles in which the observer is expected to converge. The cylinder pressure at the end of the induction stroke is initially different for the four cylinders, due to the simulated air charge maldistribution. After the controller is switched on, however, final cylinder pressure is quickly equalized in all cylinders.

It is worthwhile to point out that if, instead of a manifold pressure sensor, an air flow meter in the throttle body is used, the model is truly *unobservable* at low engine speeds (N < 1500). Typically in that case, the manifold pressure is lower than 7psi. Recalling that the ambient pressure is 14.7 (i.e., $\frac{p_{amb}}{p_{man}} > 2$), it is immediately clear that the air flow into the intake manifold is choked (constant), being governed only by geometric characteristics, and hence any manifold pressure fluctuations go unnoticed by the air flow meter. This implies of course, that individual cylinder pressure control is not possible at lower engine speeds if only air flow data are available.

REFERENCES

[1] D. Broome (1969), "Induction ram", *Automobile Engineer*, Part I, April, pp. 130-133; Part II, May, pp. 180-184; Part III, June, pp. 262-267.

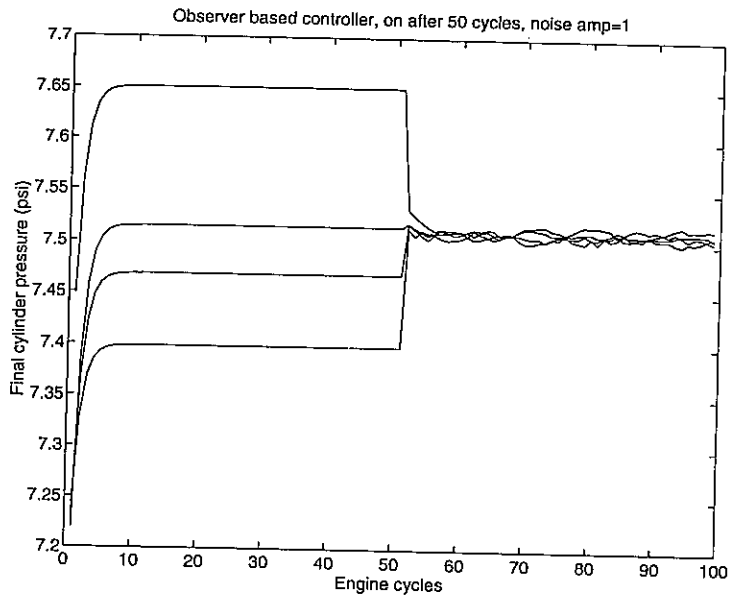

Figure 9: Observer based controller at 1500 RPM.

[2] J.W. Grizzle, J.A. Cook, and W.P. Milam, "Improved cylinder air charge estimation for transient air fuel ratio control," *Proceedings of the 1994 American Control Conference*, Baltimore, 1994, pp.1568–1573.

[3] J. Heywood (1988), *Internal combustion engine fundamentals*, McGraw Hill, 1988.

[4] P.E. Moraal, J.W. Grizzle and J.A. Cook, "An observer design for single-sensor individual cylinder pressure control", *Proceedings of the IEEE CDC*, San Antonio, 1993, pp.2955–2961.

[5] P.E. Moraal and J.W. Grizzle, "Observer design for nonlinear systems with discrete-time measurements," to appear in *IEEE Transactions on Automatic Control*, 1995.

[6] R.J. Pearson and D.E. Winterbone, "A rapid wave action simulation technique for intake manifold design", *SAE paper* No. 900676, 1990.

[7] B. K. Powell, "A dynamic model for automotive engine control analysis," *Proceedings of the 18th IEEE Conference on Decision and Control*, 1979, pp. 120–126.

[8] B. K. Powell and J. A. Cook, "Nonlinear low frequency phenomenological engine modelling and analysis," *Proc. of the American Control Conference,* Minneapolis, MN, 1987, pp. 332–340.

[9] M.P. Thompson and H.W. Engelman (1969), "The two types of resonance in intake tuning", ASME 69-DGP-11, 1969.